Atmos. Chem. Phys. Discuss., https://doi.org/10.5194/acp-2018-151
Manuscript under review for journal Atmos. Chem. Phys.
Discussion started: 19 February 2018
© Author(s) 2018. CC BY 4.0 License.

Atmospheric Chemistry and Physics Discussions

Occurrence and Spatial Distribution of the Neutral Per-fluoroalkyl Substances, and Cyclic Volatile Methylsiloxanes in Atmosphere of the Tibetan Plateau

Xiaoping Wang[1,2*], *Jasmin Schuster*[3,4], *Kevin C. Jones*[4], *and Ping Gong*[1,2]

[1]Key Laboratory of Tibetan Environment Changes and Land Surface Processes, Institute of Tibetan Plateau Research, Chinese Academy of Sciences, Beijing, 100101, China

[2]CAS Center for Excellence in Tibetan Plateau Earth Sciences，Beijing, 100101, China

[3]Air Quality Processes Research Section, Environment and Climate Change Canada, 4905 Dufferin St., Toronto, ON M3H 5T4, Canada

[4]Lancaster Environment Centre, Lancaster University, Lancaster, LA1 4YQ, U.K.

*** Corresponding author address:**

E-mail: wangxp@itpcas.ac.cn

Tel: +86-10-84097120

Fax: +86-10-84097079

Atmos. Chem. Phys. Discuss., https://doi.org/10.5194/acp-2018-151
Manuscript under review for journal Atmos. Chem. Phys.
Discussion started: 19 February 2018
© Author(s) 2018. CC BY 4.0 License.

Atmospheric Chemistry and Physics Discussions

Abstract

Due to their properties of bioaccumulation, toxicity, and long-range atmospheric transport, poly and per-fluoroalkylsubstances (PFASs), and cyclic volatile methyl silxoanes (cVMS) are currently being considered as emerging persistent organic pollutants (POPs) for regulation. To date, there are limited data on PFASs and cVMS in the atmosphere of the Tibetan Plateau (TP), a remote environment which can provide information on global background conditions. Sorbent-impregnated polyurethane foam (SIP) disk passive air samplers were therefore deployed for three months (May to July 2011 and 2013) at 16 locations across the TP. Using previously reported methods for estimating the air volume sampled by SIP disks, the derived atmospheric concentrations ranged as follows: 18–565 ng/m^3 for ΣcVMS (including D3, D4, D5, and D6); 65–223 pg/m^3 for fluorotelomer alcohols (ΣFTOHs); 1.2–12.8 pg/m^3 for fluorinated sulfonamides (ΣFOSA); and 0.29–1.02 pg/m^3 for fluorinated sulfonamidoethanols (ΣFOSE). The highest ΣcVMS occurred at Lhasa, the capital city of the TP, indicating the local contribution to the emerging pollutants. Higher levels of ΣFTOHs were observed at sites close to the transport channel of the Yarlung Tsangpo Grand Canyon, indicating possible long-range atmospheric transport (LRAT). Elevated concentrations of shorter-chain volatile PFAS precursors (4:2 FTOH and fluorobutane sulfonamidoethanol) were found in most air samples, reflecting the shift in production from long- to short-chain PFASs in Asia. Overall, concentrations of emerging POPs at background sites of the TP were 1–3 orders of magnitude higher than those reported for legacy POPs.

Atmos. Chem. Phys. Discuss., https://doi.org/10.5194/acp-2018-151
Manuscript under review for journal Atmos. Chem. Phys.
Discussion started: 19 February 2018
© Author(s) 2018. CC BY 4.0 License.

45 **Introduction**

46 Persistent organic pollutants (POPs) have attracted significant attention due to their
47 wide distribution in the environment and high toxicity to humans and wildlife (Hung et
48 al., 2016a; Hung et al., 2016b; Magulova and Priceputu, 2016; Rigét et al., 2010). In
49 the first stage, the Stockholm Convention included twelve POPs, normally considered
50 the legacy POPs (Rigét et al., 2010), including dichlorodiphenyltrichloroethane (DDT),
51 hexachlorobenzene (HCB), and hexachlorocyclohexanes (HCHs). With the prohibition
52 of these legacy POPs, their levels in the environment have largely deceased (Hung et
53 al., 2016a; Hung et al., 2016b). Compared with these legacy POPs, other organic
54 substances, such as per-fluoroalkyl substances (PFASs), and volatile methyl-siloxanes
55 (VMS), have attracted more attention in recent years in the environmental chemistry
56 research community (Pedersen et al., 2016; Shi et al., 2015; Wang et al., 2015a; Xiao
57 et al., 2015) due to their widespread production, bioaccumulative behavior, and toxicity.
58 In 2009, perfluorooctanesulfonic acid (PFOS) and perfluorooctane sulfonyl fluoride
59 (POSF)-based chemicals were listed under Annex B of the restricted substances of the
60 Stockholm Convention (Zushi et al., 2012).

61 In addition, use of VMS in personal care products have also been restricted by the
62 European Chemical Agency. Due to their widespread use in inks, waxes, firefighting
63 foams, metal plating and cleaning, coating formulations, and repellents for leather,
64 paper, and textiles, large quantities of PFASs have been discharged into the
65 environment (Shoeib et al., 2006). Taking PFOS as an example, the total historical
66 worldwide production of "PFOS equivalent", including secondary reaction products
67 and precursors, was estimated to be 122,500 tons between 1970 and 2002 (Guerranti et
68 al., 2013; Paul et al., 2009). However, since 2002, the emission of PFASs has shifted
69 from North America, Europe, and Japan to emerging Asian economies, especially
70 China and India (Li et al., 2011; Sharma et al., 2016). Passive air sampling results have
71 found that fluorotelomer alcohols (FTOH) and fluorinated telomere olefins (FTO) are
72 major congeners occurring in the urban air of China and Japan, while 4:2 FTOH is a

© Author(s) 2018. CC BY 4.0 License.

73 predominant chemical in remote regions of China and India (Li et al., 2011).

74 Methylsiloxanes are widely used in industrial and commercial applications, including
75 additives in fuel, car polish, cleaners, waxes, and personal care products (cosmetics,
76 deodorants and lotions, Borga et al., 2013; Buser et al., 2013). Cyclic volatile
77 methylsiloxanes (cVMS) include hexamethylcyclotrisiloxane (D3),
78 octamethylcyclotetrasiloxane (D4), and their rearrangement products such as
79 decamethylcyclopentasiloxane (D5) and dodecamethylcyclohexasiloxane (D6). These
80 chemicals are the subject of increasing concern because of their high emissions, long
81 persistence (Navea et al., 2011), and toxicities (Mackay et al., 2015). D4 and D5 have
82 been categorized as high production volume chemicals (McLachlan et al., 2010) and
83 identified as new persistent and bioaccumulative chemicals in commerce (Borga et al.,
84 2013; McGoldrick et al., 2014). Due to the high volatility, VMS can be released into
85 the atmosphere during use and production (Xu et al., 2014). The half-lives of VMS in
86 the atmosphere range from days to weeks (Xu et al., 2014; Xu and Wania, 2013), which
87 allow them to undergo long-range atmospheric transport (LRAT) and arrive at remote
88 regions such as the Arctic and Antarctic.

89 Despite of the minor local emissions, remote regions can also receive pollutants by
90 LRAT and the contamination levels of pollutants in these areas reflect the extent to
91 which the remote area has been contaminated. Studies on the occurrence and
92 distribution of PFASs and cVMS have been conducted in various environmental media
93 of the Arctic (Krogseth et al., 2013) and Antarctic (Sanchís et al., 2015), where
94 unexpectedly high concentrations were found. As well as the Arctic and Antarctic, the
95 Tibetan Plateau (TP) is often referred to as the “third pole”, isolated in the mid-latitude
96 northern hemisphere with a harsh environment and high elevation. The transport (Sheng
97 et al., 2013), distribution (Wang et al., 2010; 2016b), and bioaccumulation (Ren et al.,
98 2016) of legacy POPs in the Tibetan environment have already been investigated;
99 however, there is still a gap in knowledge regarding the distribution of emerging
100 organic contaminants, such as PFASs and cVMS.

Atmos. Chem. Phys. Discuss., https://doi.org/10.5194/acp-2018-151
Manuscript under review for journal Atmos. Chem. Phys.
Discussion started: 19 February 2018
© Author(s) 2018. CC BY 4.0 License.

Atmospheric Chemistry and Physics Discussions

In this study, sorbent-impregnated polyurethane foam (SIP) disk passive air samplers were deployed across the TP (16 sites) to obtain the spatial distribution of PFASs and cVMS in the atmosphere. These sites include densely populated cities and background sites, in order to test how the local emission and LRAT contaminate the TP. Combining the results of this study with the published data regarding legacy POPs in the TP, and emerging POPs in other Asian regions, will provide useful insights to help rank the exposure risks of legacy and emerging POPs in the Tibetan environment, and gain a comprehensive understanding of the distribution pattern of emerging POPs in Asia.

Materials and methods

Preparation of SIPs. Air monitoring in remote areas is especially challenging due to the lack of electricity. Passive air samplers (PAS) have the advantage that they do not require electricity, and are also cheap and easy to handle. Among the various PAS, SIP uses polyurethane foam (PUF) coated with polystyrene divinylbenzene copolymeric resin (XAD-4) as the absorption medium, which has been widely used for a range of POPs, including PFASs, VMS, and PCBs (Ahrens et al., 2013; Genualdi et al., 2010, 2011; Shoeib et al., 2008). The preparation of SIP was conducted at Lancaster University, U.K., following the previously published method (Shoeib et al., 2008). Briefly, PUF disks (Tisch Environmental) were pre-extracted in a Soxhlet with acetone (12 h) and petroleum ether (18 h). Amberlite XAD-4 was precleaned by sonication in methanol, dichloromethane, and hexane (30 min each). The precleaned Amberlite XAD-4 was ground to a powder using a Retsch planetary ball mill (particle diameter approximately 0.75 μm). The PUF disks were coated with the XAD-4 by dipping the precleaned disks in a dispersion of the powdered Amberlite XAD-4 slurry in hexane. SIP-PUF disks were dried under vacuum, and an average of 435 ± 30 mg of XAD-4 coated each disk (n = 80; each sampling had 32 samples and 8 field blanks), which was similar to the Global Passive Atmospheric Sampling program (Genualdi et al., 2010). All prepared SIP disks were stored in sealed metal tins at −17°C until they were transferred to the sampling locations.

Atmos. Chem. Phys. Discuss., https://doi.org/10.5194/acp-2018-151
Manuscript under review for journal Atmos. Chem. Phys.
Discussion started: 19 February 2018
© Author(s) 2018. CC BY 4.0 License.

129 **Sampling campaign**

130 Taking advantage of the Tibetan Observation and Research Platform (Wang et al.,
131 2016a), a passive air monitoring network comprising 16 sampling sites across the TP
132 has been established, with good spatial coverage of the TP (Supporting Information,
133 Fig. S1), and has already produced results regarding the spatial and temporal pattern of
134 legacy POPs (Wang et al., 2010; 2016b). In this study, duplicate SIP-PAS were
135 deployed at each sampling site for about 100 days from May to July for sampling
136 PFASs (2011) and cVMS (2013). During the sampling, another PUF sampler was co-
137 deployed to obtain the site-specific sampling rate using four depuration compounds
138 (DCs; PCB-30, -54,-104, and -188; Pozo et al., 2009). Details relating to the DCs can
139 be found in Text S1. The sampling program and meteorological conditions at each site
140 are provided in Table 1. Field blanks were unpacked and exposed them in air for 1 min
141 at the sampling site and then treated as real samples. At the end of the deployment
142 period, the collected SIP-PUF and PUF disks were sealed in metal tins and transported
143 to the clean lab in Lhasa for extraction.

144 **Sample extraction and analysis**

145 The target PFASs were neutral PFASs, including fluorotelomer olefin (8:2 FTO),
146 fluorotelomer acrylates (6:2, 8:2 FTA), fluorotelomer alcohols (4:2, 6:2, 8:2, 10:2, and
147 12:2 FTOH), sulfonamides (NMeFBSA, NMeFOSA, and NEtFOSA), and
148 sulfonamidoethanols (NMeFBSE, NMeFOSE, and NEtFOSE); the four target cVMS
149 were D3, D4, D5, and D6. PFAS standards were purchased from Wellington
150 Laboratories Inc. (Guelph, Ontario, Canada), and D3, D4, D5, and D6 were purchased
151 from Tokyo Chemical Industries America (Portland, OR).

152 Extraction of the PFASs was performed by sequential cold column extraction with ethyl
153 acetate as the extraction solvent. Field blanks and lab blanks were extracted along with
154 samples in the same way. After the spiking of the recovery standard (see Table S1 for
155 the composition), SIP was extracted by three separate immersions (30 min) in ethyl

© Author(s) 2018. CC BY 4.0 License.

acetate, and all three extracts were combined and concentrated. These extracts were then filtered by Millipore Millex syringe filter unite (0.45μm, 4mm), reduced to a volume of 1 ml and cleaned up by 2 cm of Envi-Carb. Finally, after adding the internal standard (Table S1), the extracts were reduced to 50 μl for injection. The analysis of volatile PFASs was performed using GC-MS equipped with a SUPELCO WAX column (60 m, 0.25 mm inner diameter, 0.25 μm film, Supelco, Bellefonte, PA) under positive chemical ionization mode.

Before sampling, the SIP disks were spiked with recovery mixture containing each of the ^{13}C4-D4, ^{13}C5-D5, and ^{13}C6-D6, and after sampling, they were Soxhlet extracted with petroleum ether/acetone (85/15, v/v) for around 6 h. All extracts were then concentrated by rotary evaporation, followed by gentle nitrogen blow-down to 0.5 mL using isooctane as a keeper for the extracts. Mirex was added to the final extract as an internal standard. The separation and detection of the cVMSs was performed using GC-MS in selective ion monitoring mode using a DB-5 column (60 m, 0.25 mm inner diameter, 0.25 μm film, J&W Scientific).

Quality assurance/quality control

Samples were extracted in a clean lab with filtered, charcoal stripped air and positive pressure conditions. All glassware used for sample collection was cleaned, and baked at 450°C before use. Powder-free nitrile gloves were used for all handling of the samples. All personnel involved in sample collection and analysis refrained from using personal care products to avoid contamination. A total of eight field blanks and six lab blanks were analyzed for target PFASs. In the lab blanks, only 8:2 FTOH and 10:2 FTOH were screened, which showed low concentrations, while 4:2 FTOH, 8:2 FTOH, 10:2FTOH, NEtFOSA, NMeFOSE, and NEtFOSE were observed in field blanks, with concentrations ranging between 50 and 321 pg/sample (Table S2). Similarly, eight field blanks and six lab blanks were arranged for evaluating the uncertainties of cVMS concentrations due to contamination and loss processes (during the extraction and cleanup procedures and storage). D3, D4, D5, and D6 in field blanks were, on average,

© Author(s) 2018. CC BY 4.0 License.

34, 57, 380, and 59 ng/sample, respectively, which were approximately 6% of the sample concentration. Method detection limits (MDLs) were calculated from the blanks [average of blanks + 3 × standard deviation (σ)]. Based on this principle, MDLs of volatile PFASs ranged between 37 and 419 pg/sample, while MDLs of cVMS ranged between 52 and 681 ng/sample (Table S3). Details of the MDLs for each congener are provided in Table S2 and S3.

The average recoveries were 88 ± 27%, 79 ± 34%, 71 ± 27%, 95 ± 21%, and 107 ± 19% for 5:1 FTOH, 7:1FTOH, [M+5]8:2 FTOH, 9:1 FTOH, and 11:1 FTOH, respectively; and 117 ± 33%, 105 ± 27%, 89 ± 37%, 93 ± 33%, and 92 ± 29% for [M+3]NMeFOSA, [M+5]NEtFOSA, [M+7]NMeFOSE, and [M+9]NEtFOSE, respectively. These recoveries were broadly in line with previous passive air sampling for Asian counties in which the same SIP disks were deployed (Li et al., 2011). The recoveries were 116.0 ± 5.9%, 90 ± 8.5%, and 98.2 ± 1.7% for ^{13}C-D4, ^{13}C-D5, and ^{13}C-D6, respectively. Recoveries over 100% were observed for ^{13}C-D4, which may be due to transformation to ^{13}C-D4 from ^{13}C-D5 during sampling (~100 days) and storage.

Sampling rate calculation

Generally, the uptake profile of a chemical to the passive sampler medium (PSM) includes three stages: 1) quick, linear uptake when the amount of chemicals in the PSM is small; 2) curvilinear uptake (slow uptake); and 3) equilibrium uptake when the amount of chemicals in the PSM reaches a plateau. Volatile compounds usually have short linear phase absorption and equilibrate after a few weeks in SIP (Ahrens et al., 2013; Shoeib et al., 2008), while longer linear phases will occur if SIP is operated at colder temperatures (Ahrens et al., 2013). In a previous calibration study (in which the sampling temperature was 18°C), linear phase uptake of PFASs in SIP was reported (Ahrens et al., 2013), due to the greater capacity of SIP-PAS to PFASs. However, the sampling temperature in the present study (Table 1) was much lower, and so linear phase absorption should be expected to occur. For this reason, the previously reported average linear sampling rate (R) of 4 m^3d^{-1} reported by Ahrens et al (2013) for PFASs

Atmos. Chem. Phys. Discuss., https://doi.org/10.5194/acp-2018-151
Manuscript under review for journal Atmos. Chem. Phys.
Discussion started: 19 February 2018
© Author(s) 2018. CC BY 4.0 License.

Atmospheric Chemistry and Physics Discussions

(including FTOHs, FOSAs and FOSE) was chosen to estimate the final sample air volume of the SIP-PAS (multiplying 4 m^3d^{-1} by the number of days of deployment). Based on this estimation, volumetric concentrations of target compounds were obtained and are presented in Table S4. The MDLs in Table S4 were also calculated based on the 90-day exposure duration.

The volume of air sampled for cVMS in SIP disks can be described by the following equation:

$$V_{air} = K_{SIP-A} \times V_{SIP} \times (1 - \exp\{-(A_{SIP})/(V_{SIP}) \times (k_A/K_{SIP-A})\}t) \quad (1)$$

where V_{air} is the air volume sampled by the SIP disk, $K_{SIP\text{-}A}$ is the SIP-air partition coefficient, V_{SIP} is the volume of the SIP disk (cm^3), A_{SIP} is the planar surface area of the SIP disk (cm^2), k_A is the air-side mass transfer coefficient (m/day), and t is deployment time (days). $K_{SIP\text{-}A}$ is highly temperature dependent and can be calculated using its correlations with K_{OA} (Ahrens et al., 2014). Details about the calculation are presented in Table S5. Values of k_A can be derived from the site-specific sampling rate (Rs) and the surface area of the SIP disk (A_{SIP}). The Rs values were calculated from the use of DCs on the PUF disks that were co-deployed at each site. Details of these calculations have been previously reported and are presented in Text S2 and Table S6. The values of log ($K_{SIP\text{-}A}$) for D3, D4, D5, and D6 are listed in Table S7; and the air volume sampled by the SIP disk are provided in Table S8. Then, volumetric concentrations of D4, D5, and D6 are presented in Table S9.

Result and discussion

Concentration of neutral PFASs and cVMS

From Table S5, with the exception of fluorotelomer acrylates (6:2, 8:2 FTA), all neutral PFAS congeners were quantitatively detected in all samples. This implies that the neutral PFAS were ubiquitous in the air of the TP. The dominant compounds were FT alcohols, with the total concentration of FTOH (sum of 4:2 FTOH, 6:2 FTOH, 8:2

Atmos. Chem. Phys. Discuss., https://doi.org/10.5194/acp-2018-151
Manuscript under review for journal Atmos. Chem. Phys.
Discussion started: 19 February 2018
© Author(s) 2018. CC BY 4.0 License.

Atmospheric Chemistry and Physics Discussions

FTOH, 10:2 FTOH and 12:2 FTOH) ranging from 65 to 223 pg/m^3. These values are lower than those measured in Chinese cities, such as Beijing, Taiyuan, and Changsa (Li et al., 2011) but are higher than those reported at background sites, including remote mountains in China (80–120 pg/m^3, Li et al., 2011), Antarctica (13.5–46.9 pg/m^3, Wang et al., 2015b), and the Arctic (7.7–49 pg/m^3, Shoeib et al., 2006). Among all the FTOHs, concentrations of 8:2 and 4:2 FTOH were the highest, being in the tens of (up to one hundred) pg/m^3. Generally, 8:2 FTOH was the prevailing compound found in the gas phase. This may be due to its relatively high volatility and long atmospheric lifetime (Rayne et al., 2009). However, concentrations of 8:2 FTO were in the range of 0.88 to 4.56 pg/m^3, which are lower than those measured in other background regions (~ tens of pg/m^3, Li et al., 2011). Levels of fluorinated sulfonamides (sum of NMeFBSA, NMeFOSA, and NEtFOSA) in Table S4 can reach a maximum of around 10 pg/m^3, while the total concentration of sulfonamidoethanols (including NMeFBSE, NMeFOSE, and NEtFOSE) was only a few pg/m^3, which is an order of magnitude lower than those observed for sulfonamides. It is clear that the proportion of FTOHs was much higher than FOSEs and FOSAs, which may be due to FOSEs and FOSAs being prone to absorption on particles (Li et al., 2011).

The measurements reported here represent the first survey of concentrations of cVMS in the TP (also known as “the Third Pole”, Qiu, 2008). All measured cVMS concentrations were above the MDL, suggesting cVMS were also ubiquitous in the Tibetan atmosphere (Table S6). The average atmospheric concentrations for D3, D4, D5, and D6 were 29.1, 38.8, 88.6 and 1.6 ng/m^3, respectively (Table S9). Concentrations of D5 were higher than D3 and D4, which is different from the reported concentrations of 17, 16, 4.0, and 0.54 ng/m^3 for D3, D4, D5, and D6 at the Zeppelin observatory (Arctic) using the same SIP-disks for sampling (Genualdi et al., 2011). However, similar to other Arctic results, D5 was the dominant congener in air (Krogseth et al., 2013). D5 is the most frequently used cVMS in personal care products, and therefore is the predominant cVMS in the urban atmosphere (McLachlan et al., 2010). However, dominance of D5 have been observed in both Arctic and Antarctic region,

Atmos. Chem. Phys. Discuss., https://doi.org/10.5194/acp-2018-151
Manuscript under review for journal Atmos. Chem. Phys.
Discussion started: 19 February 2018
© Author(s) 2018. CC BY 4.0 License.

highlighting its persistence in atmosphere and LRAT potential. The obtained cVMS concentrations in the TP are higher than those reported for Arctic and remote Sweden, indicating the possible local contamination. Both PFASs and cVMS are closely associated with human activities, and their concentrations usually show positive correlations with population (Genualdi et al., 2010; Nguyen et al., 2016). Therefore, we would expect high concentrations of volatile PFASs and cVMs in the atmosphere of Lhasa and Golmud, which are the two largest cities on the TP, with relatively large populations and fast urbanization. From Table S4 and S9, in Lhasa (the capital and also the largest city of the Tibet autonomous region), the concentrations of 8:2 FTOH and 4:2 FTOH were 71 and 43 pg/m^3, respectively, and similar levels were also found for Golmud. Additionally, concentrations of D5 in Lhasa and Golmud were 465 and 208 ng/m^3 respectively, which were the two highest D5 concentrations in the Tibetan atmosphere (Table S10). Although these levels were still orders of magnitude lower than those reported for other megacities (Genualdi et al., 2010; Mackay, 2015) the elevated concentrations suggest that the expansion/development of cities, followed by the migration of rural populations, may lead to an increase of emerging pollutants in Tibet.

Spatial distribution and congener profile of neutral PFASs

An important objective of this study was to improve knowledge on the spatial patterns of emerging POPs in the background air across the TP. In previous studies, the spatial distributions of atmospheric legacy organochlorine pesticides over the TP have been reported, and were found to be strongly related to the air circulation patterns of the TP, i.e. the Indian Monsoon and westerly winds (Figure S2, Wang et al., 2010; 2016b). For example, DDT-related chemicals were major chemicals in the atmosphere of the southeastern TP, which is influenced by the Indian monsoon air masses (Wang et al., 2010); whereas, the northwestern TP was dominated by HCB in the atmosphere, caused by the westerly-driven European air masses (Wang et al., 2016b). Similarly, ice cores collected in different regions of the TP indicated that PFOS existed in the Muztagata glacier (western TP); while in the Zuoqiupu glacier, located in the eastern TP, PFOS

© Author(s) 2018. CC BY 4.0 License.

296 was below the detection limit, but concentrations of short-chain perfluorobutanoic acid
297 have increased during recent years (Wang et al., 2014). All these results suggest that
298 differences in the concentrations and composition profiles of POPs likely reflect the
299 upwind sources affecting the different parts of the TP (e.g., European/central Asian
300 sources for the west TP and Indian sources for the east TP).

301 Figure 1 presents the spatial patterns of 8:2 FTO, FTOHs, FOSAs, and FOSEs. The
302 spatial distribution of 8:2 FTO shows a decreasing gradient from the east to the west of
303 the TP (Figure 1). On the basis of the ANOVA results, significantly high values of 8:2
304 FTO were found at Qamdo and Bomi (Table S10). However, spatial variation was
305 found in total FTOHs (Figure 1), and significant differences only occurred at the east
306 regions (Chayu, Rawu, and Lulang) and the western sites (Gar and Muztagata, Table
307 S7). It is noted that the highest ΣFTOH concentration occurred at Chayu (222 pg/m^3),
308 which is on the southern slopes of the Himalaya and close to the China–India border.
309 Levels of ΣFTOHs in Chayu were even higher than that of Lhasa (180 pg/m^3),
310 suggesting that the southeast part of the TP may receive considerable inputs of PFASs
311 from south Asia. Regarding ΣFOSAs and ΣFOSEs, higher levels were seen in both the
312 east and west of the TP (Figure 1), compared to the middle of the TP. A previous study
313 observed high levels of atmospheric DDTs at sites (e.g. Chayu, Rawu, Bomi, etc.) close
314 to the Yarlung Tsangpo Grand Canyon (Wang et al., 2016b). Here, ΣFTOHs, ΣFOSAs,
315 and ΣFOSEs also showed higher levels at these sites (Figure 1), which confirms
316 previous results that show that the Yarlung Tsangpo Grand Canyon is a channel for
317 receiving pollutants from southern Asia (Sheng et al., 2013; Wang et al., 2016b).
318 Medium ΣFOSA and ΣFOSE concentrations found in the Muztagata region broadly
319 agree with the previous results that air masses originating from European sources are
320 generally clean (Wang et al., 2016b).

321 As mentioned above, the composition profile of POPs is closely associated with air
322 circulation patterns in the TP and can reflect the upwind sources. However, congener
323 profiles of neutral PFASs in this study did not show any clear difference between
324 western sites (e.g. Muztagata, Gar) and eastern sites (Chayu, Bomi, Lulang, etc.)

© Author(s) 2018. CC BY 4.0 License.

(Figure 1), which may be because the sampling period was too short (~ 3 months) and only covered the monsoon season (June to September). Elevated 4:2 FTOH and NMeFBSE concentrations were found in most of the samples of the present study and a dominance of shorter-chain volatile PFAS precursors was the feature of the south Asian sources (Li et al., 2011). This similarity suggests that neutral PFASs in the TP may originate mainly from south Asia, most likely by LRAT.

Although the congener profiles cannot be used to distinguish the European and Indian sources in this study, the ratio of 8:2 to 10:2 to 6:2 FTOH is an excellent indicator of LRAT for atmospheric PFASs (Wang et al., 2015b). The transport fate of atmospheric PFASs can be influenced by photochemical degradation. A higher ratio indicates the aged nature of the air mass because of the fast photochemical degradation of 6:2 FTOH (half-life = 50 days) in the air compared with 10:2 FTOH (70 days) and 8:2 FTOH (80 days, Piekarz et al., 2007). During LRAT, more 6:2 and 10:2 FTOH will be removed from the atmosphere. For example, ratios of 6.4:2.1:1.0 were observed in the Arctic (Ahrens et al., 2011) and 35.6:6.5:1.0 were found in the Antarctic (Wang et al., 2015b). In the present study, low ratios were observed in the cities, i.e. 2.4:1.7:1 and 6.8:1.2:1 were observed for Lhasa and Golmud, respectively. This indicates that cities are possible fresh emission sources of neutral PFASs. According to a previous study, there are three climate zones over the TP—namely, the monsoon region, westerly region, and transition region (Wang et al., 2016b). The sampling sites of this study can be grouped into these three zones (Figure S2, Table S11). The average ratios of 8:2 to 10:2 to 6:2 FTOH were 8.4:1.2:1 for the monsoon region, 8.8:1:1 for the westerly region and 10.6:1.2:1 for the transition zone (Figure S2, Table S11). Overall, these values are comparable to those reported for the Arctic. On the other hand, a decrease in 6:2 FTOH and an increase in 8:2 and 10:2 FTOH occurred from the edge regions to the central part of the TP (Table S11). The high ratios indicate the aged nature of atmospheric PFASs in the atmosphere of the TP, especially around the transition zone (Table S11). Given that the transition zone is located in the hinterland (central part) of Tibet, relatively far away from the source regions of either India or Europe/central Asia, the

© Author(s) 2018. CC BY 4.0 License.

aged PFASs in the air of central TP is expected and reasonable.

Correlations between PFAS compounds

Correlations between concentrations of pollutants can be used to test if they have some common sources or undergo similar environmental fates. A correlation matrix was therefore prepared and showed that some chemicals were significantly correlated (Table 2). Good correlations ($r > 0.80$, $p < 0.01$) were observed between 8:2 FTOH and 10:2 FTOH ($r = 0.90$), and between 10:2 FTOH and 12:2 FTOH ($r = 0.97$). This phenomenon has been observed in other studies (Ahrens et al., 2012; Cai et al., 2012; Li et al., 2011) and usually suggests that 8:2 FTOH, 10:2 FTOH, and 12:2 FTOH have the same source. Correlations between 4:2 FTOH and other FTOHs are generally low, or not significant, indicating 4:2 FTOH may come from different sources. There is much evidence that the manufacture of PFASs has shifted from longer-chain chemicals (C8 or above) to shorter-chain ones (Butt et al., 2010; Hogue, 2012), which may lead to the poor correlation between 4:2 FTOH and other FTOHs. Given the new production of shorter-chain PFASs mainly centered in Asian countries, such as China and India (Hogue, 2012) it is not surprising that high levels of both 4:2 FTOH and its independent characteristics have been found in the Tibetan atmosphere, due to the close proximity between Tibet and south Asia.

With regard to the relationships between FOSAs and FOSEs, good correlations were seen among NMeFBSA, NMeFOSA, and NEtFOSA (Table 2). Additionally, concentrations of NMeFBSE were significantly correlated with those of NMeFOSE (Table 2). This is in contrast to previous results, in which poor relationships were found between short- and long-chain PFASs (Li et al., 2011). Regarding the emission patterns of FOSAs and FOSEs in India, mixed manufacturing with both extensive emissions of NMeFOSA and NMeFOSE, coupled with wide discharge of NMeFBSA, have been reported in the Indian environment (Li et al., 2011). This indicates that both long- and short-chain PFAS are produced in south Asia. Favored by the transport of the Indian monsoon, the co-transport of short- and long-chain PFASs may lead to a blending of

© Author(s) 2018. CC BY 4.0 License.

these chemicals in the Tibetan air. Meanwhile, the two short-chain PFASs, 4:2 FTOH and NMeFBSA, were significantly (r = 0.84, p < 0.01; Table 2) correlated with each other, suggesting these precursors may be released together in the source region.

Spatial distribution of cVMS across the TP

As mentioned above, greater levels of cVMS were found in the urban areas of Lhasa and Golmud. This can also be seen in the spatial map of cVMS (Figure 2). However, high levels of cVMS also occurred in the remote southeast of Tibet (Figure 2). Unlike the spatial pattern of neutral PFASs, concentrations of cVMS decreased from southeast to northwest TP (Figure 2, Table S9). Although there are no studies that report the cVMS levels and patterns in south Asian countries, due to the source of cVMS to the environment taking place via the use of personal care products we can expect the regions of south Asia (e.g. the Indo-Gangetic Plain), with its high population density, to be important cVMS source regions. The close proximity of the southeast TP to south Asia and the fast LRAT potential of cVMS (Xu et al., 2014; Xu and Wania, 2013) might be the reason that high concentrations of cVMS occur in the southeast TP. On the other hand, latitude might be a factor representing the influence of the emission source on the spatial pattern.

Another reason that can also influence the atmospheric concentration of cVMS is their atmospheric degradation by hydroxyl radicals. In the Arctic, low levels of hydroxyl radicals during the polar night promotes the accumulation of cVMS in the air, while the polar day enhances the degradation, causing the strong seasonality of cVMS in the Arctic (Krogseth et al., 2013). The polar day usually increases hydroxyl radicals in the air and enhances the photo-degradation of contaminants (Krogseth et al., 2013). The level of hydroxyl radicals is generally proportional to the extent of solar UV radiation (Rohrer and Berresheim, 2006). Recently, Liu et al. (2017) published two UV radiation datasets that cover the whole of China, and high values were observed for the south TP, with a gradual decrease from the south to the north TP. Although the sampling sites in their study were not exactly the same as in our study, their spatial trend of UV radiation

Atmos. Chem. Phys. Discuss., https://doi.org/10.5194/acp-2018-151
Manuscript under review for journal Atmos. Chem. Phys.
Discussion started: 19 February 2018
© Author(s) 2018. CC BY 4.0 License.

suggested that latitude might be a possible proxy to describe the variation of UV radiation over the TP. Additionally, from a global perspective, surface UV radiation increases with elevation due to the shorter distance of travel through the atmosphere (Sola et al., 2008), which may also have a negative influence on the atmospheric concentration of cVMS. Thus, elevation and latitude can be integrated together to simulate the effects of UV radiation (representing the influence of hydroxyl radicals) on concentrations of cVMS. On the other hand, latitude is also a factor that can represent the influence of emission sources; low-latitude regions will receive more cVMS due to their proximity to source regions (see Figure 2). Thus, an empirical model was derived here to estimate the combined effects of UV radiation and the distance to emission source regions on concentrations of cVMS:

$$C_{cVMS} = a + b\,Elevation + c\,Latitude \quad (2)$$

where a, b and c are coefficients determined from statistical regression. For the multiple linear regressions, the R^2 values can be used to explain the variation of the dependents. According to the correlations (the data from Lhasa and Golmud were excluded), the relationship can be described as in the following:

$$C_{cVMS} = 134 - 0.011\,Elevation - 2.35\,Latitude \quad (R^2 = 0.60, p < 0.01)$$

This means elevation and latitude can jointly explain 60% of the atmospheric concentration of cVMS. Other factors, such as cloud coverage and sky clarity (which influence hydroxyl radical levels in the air), may be the confounding factors that influence the correlation (Sola et al., 2008). The slope for elevation (b) is negative, suggesting that high concentrations of cVMS will occur at sites with low elevation, where hydroxyl radiation is limited. Two competing factors influence the coefficient for latitude. The contribution from the proximity to source regions means that the low-latitude regions of the TP will have high concentrations of cVMS (negative correlations between latitude and C_{cVMS}), due to these sites being close to the source regions of south Asia, while the strong hydroxyl degradation caused by UV radiation at low latitudes

Atmos. Chem. Phys. Discuss., https://doi.org/10.5194/acp-2018-151
Manuscript under review for journal Atmos. Chem. Phys.
Discussion started: 19 February 2018
© Author(s) 2018. CC BY 4.0 License.

would have the opposite effect of reducing the concentrations of cVMS (positive correlation between latitude and C_{cVMS}). From the above model, the slope for latitude (c) in the model is also negative (−2.35), implying that the contribution from the proximity to source regions to concentrations of cVMS is broadly greater than that of hydroxyl degradation.

Correlations between cVMS congeners

Similar to previously published studies, good correlations were found between D3, D4, and D5 (Table S9). The correlation coefficients varied from 0.69 to 0.79 (all correlations were significant at the 95% confidence level; the data from Lhasa and Golmud were excluded), while the correlation between D5 and D6 was not significant. The good correlation implies that either D3, D4, and D5 have common sources and transport mechanisms, or there is chemical transformation to D3 and D4 from D5 (Kierkegaard et al., 2010).

Comparison of Measured and Modeled D5 Concentrations.

The measured D5 concentrations are compared with the concentrations predicted by the Danish Eulerian Hemispheric Model (DEHM, McLachlan et al., 2010). The country-based emissions were distributed into the DEHM grid according to a data set of the gridded population density of the world with the total emission of D5 within the DEHM model domain estimated as 30 kT per year (McLachlan et al., 2010). All physical-chemical properties of D5 used in model prediction are reported in previous study (Brooke et al., 2009; Jiménez et al., 2005). The rate constant for the reaction of D5 with OH radicals measured by Atkinson (1991) was employed. NCEP (National Centers for Environmental Prediction) global analysis meteorological data are used to driven model. By comparing different scenarios, the DEHM model found that phototransformation is the dominant elimination process between emission of the D5 and arrival at the sampling site. There is good agreement between the spatial variability in D5 concentration between the measurements of the TP and the model prediction,

© Author(s) 2018. CC BY 4.0 License.

displaying great D5 concentrations in southeast TP. The good tracking of the measured concentration by the DEHM shows that D5 is clearly subject to LRAT, although it is also effectively removed from the atmosphere via phototransformation. However, measured D5 concentrations are 1-3 magnitudes higher than the model prediction. Given atmospheric emission data of D5 in DEHM are estimated from usage of antiperspirant and skin creams, the emission uncertainties might lead to the discrepancy between measured concentrations and model values.

Implications

To the best of our knowledge, this is the first study on atmospheric concentrations of neutral PFASs and cVMS in the TP region. Due to the remoteness of the TP, the contamination of these emerging compounds will provide insight into how and to what extent the emissions in the source regions influence these last pieces of pristine land. Levels of neutral PFASs in the air of the TP are in the hundreds of pg/m^3, and levels of cVMS are in the ng/m^3 range. These values are 2–3 times and 1–2 orders of magnitude, respectively, higher than those for legacy chemicals (such as DDT and HCHs, with maximum concentrations in the tens of pg/m^3, Wang et al., 2016b). Moreover, among the various legacy and emerging POPs in wild Tibetan fishes, the average level of ΣPFASs is the third highest (just after those of ΣDDT and ΣHCHs, Shi et al., 2015; Wang et al., 2016a). All this evidence suggests that emerging POPs should be of great concern for the environmental safety of the TP, as they are large volume production chemicals that have not been regulated in the surrounding countries. Due to the LRAT potential of volatile PFASs and cVMS, joint regulation of these emerging chemicals by south Asian counties (upwind of the TP) has been requested in order to protect the Tibetan environment. Taking data from this study and the pilot study for Asian countries (Li et al., 2011) into account, due to the growing population and the transfer of production factories from developed countries to Asian counties, Asian cities will increasingly be the sources of emerging POPs from a global perspective.

China has not strongly regulated the manufacture of PFASs or the use of personal care

© Author(s) 2018. CC BY 4.0 License.

products. Over the last ten years, extensive urbanization has occurred in China. For example, the population in Lhasa reached 90,000 in 2015, having increased by 33% from 2014. It is estimated that the population in Lhasa will reach 110,000 in 2020. Thus, emissions of emerging compounds due to urbanization will inevitably increase. Following the population expansion, wastewater treatment plants deployed in cities will not only emit volatile PFASs and cVMS into the air, but will also contaminate the TP's water bodies (i.e. rivers, wetlands, and lakes), which are precious clean water resources. Thus, the risks posed by city expansion to the burden and transport of pollutants should be of great concern. Increasingly, concern regarding the toxicity and exposure risks of PFASs and cVMS is growing among scientists and regulators. This work has important implications for policymakers in comprehensively protecting the Tibetan alpine environment and promoting sustainable development in Tibet (the water tower of Asia).

Acknowledgements. This study was supported by the National Natural Science Foundation of China (41671480 and 41222010), Youth Innovation Promotion Association (CAS2011067) and the International Partnership Program of the Chinese Academy of Sciences (Grant No. 131C11KYSB20160061).

Reference

Ahrens, L., Harner, T., and Shoeib, M.: Temporal Variations of Cyclic and Linear Volatile Methylsiloxanes in the Atmosphere Using Passive Samplers and High-Volume Air Samplers, Environ. Sci. Technol., 48, (16), 9374-9381, 2014.

Ahrens, L., Harner, T., Shoeib, M., Koblizkova, M., and Reiner, E. J.: Characterization of Two Passive Air Samplers for Per- and Polyfluoroalkyl Substances: Environ. Sci. Technol., 47, 14024-14033, 2013.

Ahrens, L., Shoeib, M., Harner, T., Lane, D. A., Guo, R., and Reiner, E. J.: Comparison of Annular Diffusion Denuder and High Volume Air Samplers for Measuring Per- and Polyfluoroalkyl Substances in the Atmosphere, Anal. Chem., 84, 1797-1797, 2012.

Ahrens, L., Shoeib, M., Vento, S. D., Codling, G., and Halsall, C.: Polyfluoroalkyl compounds in the Canadian Arctic atmosphere: Environ. Chem., 8, 399-406, 2011.

Atkinson, R.: Kinetics of the gas-phase reactions of a series of organosilicon compounds with OH and NO sub 3 radicals and O sub 3 at 297 + 2K, Environ. Sci. Technol., 25, 863–866, 1991

Borga, K., Fjeld, E., Kierkegaard, A., and McLachlan, M. S.: Consistency in Trophic Magnification Factors of Cyclic Methyl Siloxanes in Pelagic Freshwater Food

© Author(s) 2018. CC BY 4.0 License.

527 Webs Leading to Brown Trout: Environ. Sci. Technol., 47, 14394-14402, 2013.
528 Brooke, D. N., Crookes, M. J., Gray, D., and Robertson, S.: Environmental risk
529 assessment report: Decamethylcyclopentasiloxane, Environment Agency of
530 England and Wales, Bristol, 2009,.
531 Buser, A. M., Kierkegaard, A., Bogdal, C., MacLeod, M., Scheringer, M., and
532 Hungerbühler, K.: Concentrations in Ambient Air and Emissions of Cyclic
533 Volatile Methylsiloxanes in Zurich, Switzerland: Environ. Sci. Technol. 47,
534 7045-7051, 2013.
535 Butt, C. M., Berger, U., Bossi, R., and Tomy, G. T.: Levels and trends of poly- and
536 perfluorinated compounds in the arctic environment: Sci. Total Environ., 408,
537 2936-2965, 2010.
538 Cai, M., Xie, Z., Möller, A., Yin, Z., Huang, P., Cai, M., Yang, H., Sturm, R., He, J.,
539 and Ebinghaus, R.: Polyfluorinated compounds in the atmosphere along a cruise
540 pathway from the Japan Sea to the Arctic Ocean: Chemosphere, 87, 989-997,
541 2012.
542 Genualdi, S., Harner, T., Cheng, Y., MacLeod, M., Hansen, K. M., van Egmond, R.,
543 Shoeib, M., and Lee, S. C.: Global Distribution of Linear and Cyclic Volatile
544 Methyl Siloxanes in Air: Environ. Sci. Technol., 45, 3349-3354, 2011.
545 Genualdi, S., Lee, S. C., Shoeib, M., Gawor, A., Ahrens, L., and Harner, T.: Global
546 pilot study of legacy and emerging persistent organic pollutants using sorbent-
547 impregnated polyurethane foam disk passive air samplers: Environ. Sci.
548 Technol., 44, 5534-5539, 2010.
549 Guerranti, C., Perra, G., Corsolini, S., and Focardi, S. E.: Pilot study on levels of
550 perfluorooctane sulfonic acid (PFOS) and perfluorooctanoic acid (PFOA) in
551 selected foodstuffs and human milk from Italy: Food Chem. 140, 197-203, 2013.
552 Hogue, C.: Perfluorinated Chemical Controls: Chem. Engin. News, 90, 24-25, 2012.
553 Hung, H., Katsoyiannis, A. A., Brorström-Lundén, E., Olafsdottir, K., Aas, W., Breivik,
554 K., Bohlin-Nizzetto, P., Sigurdsson, A., Hakola, H., Bossi, R., Skov, H., Sverko,
555 E., Barresi, E., Fellin, P., and Wilson, S.: Temporal trends of Persistent Organic
556 Pollutants (POPs) in arctic air: 20 years of monitoring under the Arctic
557 Monitoring and Assessment Programme (AMAP): Environ. Pollut., 217, 52-61,
558 2016a.
559 Hung, H., Katsoyiannis, A. A., and Guardans, R.: Ten years of global monitoring under
560 the Stockholm Convention on Persistent Organic Pollutants (POPs): Trends,
561 sources and transport modelling: Environ. Pollut., 217, 1-3, 2016b.
562 Jiménez, E., Ballesteros, B., Martínez, E., and Albaladejo, J.: Tropospheric reaction of
563 OH with selected linear ketones: kinetic studies between 228 and 405 K:
564 Environ. Sci. Technol., 39, 814-820, 2005.
565 Kierkegaard, A., Adolfsson-Erici, M., and McLachlan, M. S.: Determination of Cyclic
566 Volatile Methylsiloxanes in Biota with a Purge and Trap Method: Anal. Chem.,
567 82, 9573-9578, 2010.
568 Krogseth, I. S., Kierkegaard, A., McLachlan, M. S., Breivik, K., Hansen, K. M., and
569 Schlabach, M.: Occurrence and Seasonality of Cyclic Volatile Methyl Siloxanes
570 in Arctic Air, Environ. Sci. Technol.47, 502-509, 2013.

© Author(s) 2018. CC BY 4.0 License.

571 Li, J., Vento, S. D., Schuster, J., Zhang, G., Chakraborty, P., Kobara, Y., and Jones, K.
572 C.: Perfluorinated Compounds in the Asian Atmosphere, Environ. Sci. Technol.,
573 45, 7241-7246, 2011.
574 Liu, H., Bo, H. U., Wang, Y., Liu, G., Tang, L., Dongsheng, J. I., Bai, Y., Bao, W.,
575 Chen, X., and Chen, Y.: Two Ultraviolet Radiation Datasets that Cover China,
576 Adv. Atmos. Sci., 34, 805-815, 2017.
577 Mackay, D.: Risk assessment and regulation of D5 in Canada: Lessons learned: Environ.
578 Toxicol. Chem., 34, 2687-2688, 2015.
579 Mackay, D., Powell, D. E., and Woodburn, K. B.: Bioconcentration and Aquatic
580 Toxicity of Superhydrophobic Chemicals: A Modeling Case Study of Cyclic
581 Volatile Methyl Siloxanes: Environ. Sci. Technol., 49, 11913-11922, 2015.
582 Magulova, K., and Priceputu, A.: Global monitoring plan for persistent organic
583 pollutants (POPs) under the Stockholm Convention: Triggering, streamlining
584 and catalyzing global POPs monitoring: Environ. Pollut., 217, 82-84, 2016.
585 McGoldrick, D. J., Chan, C., Drouillard, K. G., Keir, M. J., Clark, M. G., and Backus,
586 S. M.: Concentrations and trophic magnification of cyclic siloxanes in aquatic
587 biota from the Western Basin of Lake Erie, Canada: Environ. Pollut., 186,
588 141-148, 2014.
589 McLachlan, M. S., Kierkegaard, A., Hansen, K. M., van Egmond, R., Christensen, J.
590 H., and Skjøth, C. A.: Concentrations and Fate of
591 Decamethylcyclopentasiloxane (D5) in the Atmosphere, Environ. Sci. Technol.,
592 44, 5365-5370, 2010.
593 Navea, J. G., Young, M. A., Xu, S., Grassian, V. H., and Stanier, C. O.: The atmospheric
594 lifetimes and concentrations of cyclic methylsiloxanes
595 octamethylcyclotetrasiloxane (D4) and decamethylcyclopentasiloxane (D5) and
596 the influence of heterogeneous uptake: Atmos. Environ., 45, 3181-3191, 2011.
597 Nguyen, M. A., Wiberg, K., Ribeli, E., Josefsson, S., Futter, M., Gustavsson, J., and
598 Ahrens, L.: Spatial distribution and source tracing of per- and polyfluoroalkyl
599 substances (PFASs) in surface water in Northern Europe: Environ. Pollut., 220.
600 1438-1446, 2016.
601 Paul, A. G., Jones, K. C., and Sweetman, A. J.: A first global production, emission, and
602 environmental inventory for perfluorooctane sulfonate, Environ. Sci. Technol.,
603 43, 386-392, 2009.
604 Pedersen, K. E., Letcher, R. J., Sonne, C., Dietz, R., and Styrishave, B.: Per- and
605 polyfluoroalkyl substances (PFASs) – New endocrine disruptors in polar bears
606 (Ursus maritimus)? Environ. Intern., 96, 180-189, 2016.
607 Piekarz, A. M., Primbs, T., Field, J. A., Barofsky, D. F., and Simonich, S.: Semivolatile
608 Fluorinated Organic Compounds in Asian and Western U.S. Air Masses:
609 Environ. Sci. Technol., 41, 8248-8255, 2007.
610 Pozo, K., Harner, T., Lee, S. C., Wania, F., Muir, D. C. G., and Jones, K. C.: Seasonally
611 Resolved Concentrations of Persistent Organic Pollutants in the Global
612 Atmosphere from the First Year of the GAPS Study, Environ. Sci. Technol., 43,
613 796-803, 2009.
614 Qiu, J.: China: The third pole: Nature,. 454, 393, 2008

© Author(s) 2018. CC BY 4.0 License.

615 Rayne, S., Forest, K., and Friesen, K. J.: Estimated congener specific gas-phase
616 atmospheric behavior and fractionation of perfluoroalkyl compounds: rates of
617 reaction with atmospheric oxidants, air-water partitioning, and wet/dry
618 deposition lifetimes: J. Environ. Sci. Health Part A 44, 936-954, 2009.
619 Ren, J., Wang, X., Wang, C., Gong, P., Wang, X., and Yao, T.: Biomagnification of
620 persistent organic pollutants along a high-altitude aquatic food chain in the
621 Tibetan Plateau: Processes and mechanisms: Environ. Pollut., 220, 636-642,
622 2016,
623 Rigét, F., Bignert, A., Braune, B., Stow, J., and Wilson, S.: Temporal trends of legacy
624 POPs in Arctic biota, an update: Sci. Total Environ., 408, 2874-2884, 2010.
625 Rohrer, F., and Berresheim, H.: Strong correlation between levels of tropospheric
626 hydroxyl radicals and solar ultraviolet radiation: Nature, 442, 184, 2006.
627 Sanchís, J., Cabrerizo, A., Galbán-Malagón, C., Barceló, D., Farré, M., and Dachs, J.:
628 Unexpected Occurrence of Volatile Dimethylsiloxanes in Antarctic Soils,
629 Vegetation, Phytoplankton, and Krill: Environ. Sci. Technol., 49, 4415-4424,
630 2015.
631 Sharma, B. M., Bharat, G. K., Tayal, S., Larssen, T., Bečanová, J., Karásková, P.,
632 Whitehead, P. G., Futter, M. N., Butterfield, D., and Nizzetto, L.: Perfluoroalkyl
633 substances (PFAS) in river and ground/drinking water of the Ganges River
634 basin: Emissions and implications for human exposure, Environ. Pollut., 208,
635 704-713, 2016.
636 Sheng, J., Wang, X., Gong, P., Joswiak, D. R., Tian, L., Yao, T., and Jones, K. C.:
637 Monsoon-driven transport of organochlorine pesticides and polychlorinated
638 biphenyls to the Tibetan Plateau: three year atmospheric monitoring study:
639 Environ. Sci. Technol., 47, 3199-3208, 2013.
640 Shi, Y., Xu, S., Xu, L., and Cai, Y.: Distribution, Elimination, and Rearrangement of
641 Cyclic Volatile Methylsiloxanes in Oil-Contaminated Soil of the Shengli
642 Oilfield, China, Environ. Sci. Technol., 49, 11527-11535, 2015.
643 Shoeib, M., Harner, T., Lee, S. C., Lane, D., and Zhu, J. P.: Sorbent-impregnated
644 polyurethane foam disk for passive air sampling of volatile fluorinated
645 chemicals: Anal. Chem., 80, 675-682, 2008.
646 Shoeib, M., Harner, T., and Vlahos, P.: Perfluorinated chemicals in the arctic
647 atmosphere: Environ. Sci. Technol.,40, 7577-7583, 2006.
648 Sola, Y., Lorente, J., Campmany, E., De Cabo, X., Bech, J., Redaño, A., Martí nez‐
649 Lozano, J. A., Utrillas, M. P., Alados‐Arboledas, L., and Olmo, F. J.: Altitude
650 effect in UV radiation during the Evaluation of the Effects of Elevation and
651 Aerosols on the Ultraviolet Radiation 2002 (VELETA‐2002) field campaign:
652 J. Geophy. Res. Atmos. 113, 1323-1330, 2008.
653 Wang, D.-G., Aggarwal, M., Tait, T., Brimble, S., Pacepavicius, G., Kinsman, L.,
654 Theocharides, M., Smyth, S. A., and Alaee, M.: Fate of anthropogenic cyclic
655 volatile methylsiloxanes in a wastewater treatment plant: Water Res. 72, 209-
656 217, 2015a,
657 Wang, X., Gong, P., Wang, C., Ren, J., and Yao, T.: A review of current knowledge
658 and future prospects regarding persistent organic pollutants over the Tibetan

© Author(s) 2018. CC BY 4.0 License.

659 Plateau: Sci. Total Environ., 573, 139-154, 2016a.
660 Wang, X., Gong, P., Yao, T., and Jones, K. C.: Passive air sampling of organochlorine
661 pesticides, polychlorinated biphenyls, and polybrominated diphenyl ethers
662 across the Tibetan plateau: Environ. Sci. Technol., 44, 2988-2993, 2010.
663 Wang , X., Halsall, C., Codling, G., Xie, Z. g., Xu, B., Zhao, Z., Xue, Y., Ebinghaus,
664 R., and Jones, K. C.: Accumulation of perfluoroalkyl compounds in tibetan
665 mountain snow: temporal patterns from 1980 to 2010: Environ. Sci. Technol.,
666 48, 173-181, 2014.
667 Wang, X., Ren, J., Gong, P., Wang, C., Xue, Y., Yao, T., and Lohmann, R.: Spatial
668 Distribution of the Persistent Organic Pollutants across the Tibetan Plateau and
669 Its Linkage with the Climate Systems: Five Year Air Monitoring Study: Atmos.
670 Chem. Phys. 16, 6901-6911, 2016b.
671 Wang, Z., Xie, Z., Mi, W., Möller, A., Wolschke, H., and Ebinghaus, R.: Neutral
672 poly/per-fluoroalkyl substances in air from the Atlantic to the Southern Ocean
673 and in Antarctic snow, Environ. Sci. Technol., 49, 7770-7775, 2015b.
674 Xiao, R., Zammit, I., Wei, Z., Hu, W.-P., MacLeod, M., and Spinney, R.: Kinetics and
675 Mechanism of the Oxidation of Cyclic Methylsiloxanes by Hydroxyl Radical in
676 the Gas Phase: An Experimental and Theoretical Study, Environ. Sci. Technol.,
677 49, 13322-13330, 2015.
678 Xu, S., Kozerski, G., and Mackay, D.: Critical Review and Interpretation of
679 Environmental Data for Volatile Methylsiloxanes: Partition Properties: Environ.
680 Sci. Technol., 48, 11748-11759, 2014.
681 Xu, S., and Wania, F.: Chemical fate, latitudinal distribution and long-range transport
682 of cyclic volatile methylsiloxanes in the global environment: A modeling
683 assessment: Chemosphere, 93, 835-843, 2013.
684 Zushi, Y., Hogarh, J. N., and Masunaga, S.: Progress and perspective of perfluorinated
685 compound risk assessment and management in various countries and institutes:
686 Clean Technol. Environ. Policy, 14, 9-20, 2012.

Atmos. Chem. Phys. Discuss., https://doi.org/10.5194/acp-2018-151
Manuscript under review for journal Atmos. Chem. Phys.
Discussion started: 19 February 2018
© Author(s) 2018. CC BY 4.0 License.

687

Table 1 Description of the sampling program

Sampling site	Longitude	Latitude	Elevation /m; Temperature/°C	Description	Date of sample collection	
					2011	2013
Bomi	E 95°46.167′	N 29°51.485′	2720; 8.8	Hydrological observation station, remote area	05/02–07/28	05/05–07/25
Rawu	E 96°54.745′	N 29°22.289′	4540; -2	Rural site, 20 km from Rawu Lake	05/03–07/31	05/05–07/26
Lunang	E 94°44.246′	N 29°45.908′	3330; 5.4	Meteorological station in forest region, remote area	05/02–07/28	05/05–07/31
Qamdo	E 97°08.624′	N 31°09.014′	3250; 7.6	Rural site, 50 km from farm land	05/04–07/31	05/06–07/28
Chayu	E97°29.4′	N 28°37.2′	1400; 12.4	Meteorological station, remote area	05/05–07/31	05/02–07/29
Nam Co	E 90°57.800′	N 30°46.375′	4740; -2.2	Meteorological station near the Nam Co lake, remote area	05/05–07/25	05/05–07/31
GBJD	E 93°14.478′	N 29°53.122′	3420; 6.2	Hydrological observation station, remote area	05/03–07/28	05/04–07/28
Lhasa	E 91°01.956′	N 29°38.728′	3660; 8.1	Building roof of the Lhasa campus	05/01–07/31	05/08–07/28
Lhaze	E 87°38.094′	N 29°05.405′	4020; 6.8	Meteorological station, rural site	05/02–07/31	05/04–07/27
Xigaze	E 88°53.319′	N 29°15.014′	3840; 6.6	Meteorological station, rural site	05/03–07/31	05/05–07/24
Mt. Everest	E 86°56.948′	N 28°21.633′	4300; 4.3	Meteorological station near the Mt. Everest, remote area	05/02–07/31	05/03–07/29
Saga	E 85°13.951′	N 29°19.889′	4500; 6.5	Rural site and without agriculture activities	05/07–07/25	05/06–07/28
Golmud	E 94°54.480′	N 36°23.637′	2830; 5.3	Observation station for frost soil, rural site	05/02–07/27	05/06–07/27
Naqu	E 91°58.827′	N 31°25.373′	4500; -1	Hydrological observation station, remote area	05/02–07/31	05/05–07/26
Gar	E 80°05.654′	N 32°30.116′	4300; 0.6	Meteorological station, remote area	05/06–07/31	05/03–07/27
Muztagata	E 74°50.919′	N 38°16.072′	5200; -6	Meteorological station, remote area	05/09–07/31	05/07–07/29

688

Atmos. Chem. Phys. Discuss., https://doi.org/10.5194/acp-2018-151
Manuscript under review for journal Atmos. Chem. Phys.
Discussion started: 19 February 2018
© Author(s) 2018. CC BY 4.0 License.

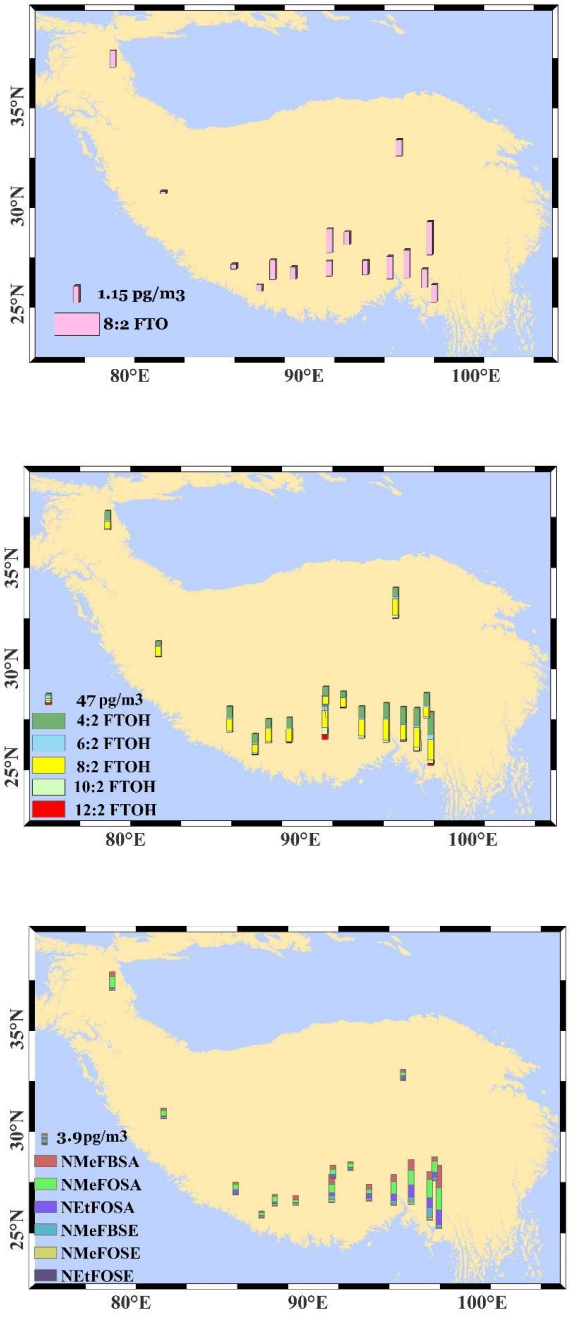

Figure 1 Spatial distribution of neutral PFASs in the atmosphere of the TP

Atmos. Chem. Phys. Discuss., https://doi.org/10.5194/acp-2018-151
Manuscript under review for journal Atmos. Chem. Phys.
Discussion started: 19 February 2018
© Author(s) 2018. CC BY 4.0 License.

Table 2 Correlation (*r*) of individual compounds among all the samples

	4:2 FTOH	6:2 FTOH	8:2 FTOH	10:2 FTOH	12:2 FTOH	NMeFBSA	NMeFOSA	NEtFOSA	NMeFBSE	NMeFOSE	NEtFOSE
8:2 FTO	0.44	0.12	0.18	0.04	0.00	0.32	0.46	0.44	0.37	0.20	−0.11
4:2 FTOH		**0.62**	0.49	0.37	0.25	**0.84**	**0.84**	**0.92**	*0.56*	0.42	−0.17
6:2 FTOH			**0.68**	*0.59*	**0.84**	**0.84**	*0.60*	*0.57*	0.39	*0.62*	−0.32
8:2 FTOH				**0.90**	0.45	**0.63**	*0.57*	*0.67*	*0.58*	**0.63**	−0.33
10:2 FTOH					**0.97**	*0.58*	0.35	0.30	0.42	**0.77**	−0.21
12:2 FTOH						*0.52*	0.26	0.19	0.33	**0.71**	−0.14
NMeFBSA							**0.83**	**0.84**	0.44	0.42	−0.24
NMeFOSA								**0.88**	**0.69**	0.43	−0.24
NEtFOSA									**0.63**	0.37	−0.03
NMeFBSE										**0.75**	−0.03
NMeFOSE											−0.13

Bold and italic are significant at $p < 0.01$ and $p < 0.05$, respectively.

Atmospheric Chemistry and Physics Discussions
Open Access
EGU

Atmos. Chem. Phys. Discuss., https://doi.org/10.5194/acp-2018-151
Manuscript under review for journal Atmos. Chem. Phys.
Discussion started: 19 February 2018
© Author(s) 2018. CC BY 4.0 License.

Atmospheric Chemistry and Physics Discussions

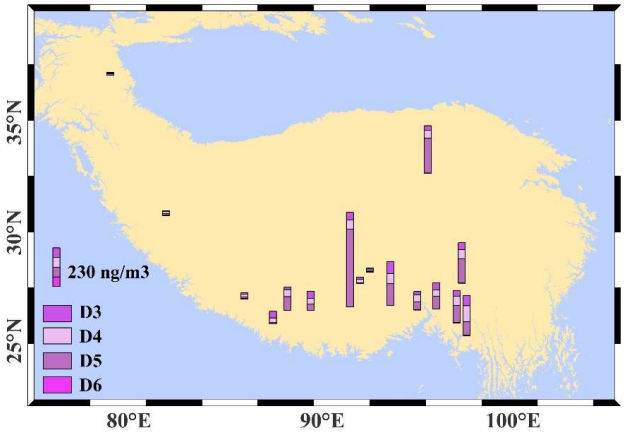

Figure 2 Spatial distribution of cVMS in the atmosphere of the TP